Aust. J. Phys., 1980, **33**, 965–73

Analysis of Angular Distributions of Heavy-ion Transfer Reactions

C. B. O. Mohr

School of Physics, University of Melbourne, Parkville, Vic. 3052.

Abstract

Proceeding as in our earlier analysis of elastic scattering, but with a form for the S matrix appropriate for transfer, peaked at the critical value l_c and with width parameter Δ, it is shown how to analyse the angular distribution of transfer reactions of heavy ions to obtain Δ. The effect of the nuclear phases is found not to be of such fundamental importance as in elastic scattering. Analysis of the experimental data reveals an increase of Δ with nuclear size especially at low energies, but an increase of nuclear penetration for transfer collisions of the lightest nuclei. The circumstances in which strong coupling might occur between elastic scattering and transfer are examined.

1. Introduction

There have been very many calculations of angular distributions of transfer reactions of heavy ions using the DWBA with optical model parameters arbitrarily adjusted to give the best fit to the experimental distributions. Yet no regular pattern has emerged as to the agreed values of these parameters for various pairs of nuclei, and the approach has provided little insight into the transfer process.

There is an alternative approach (see e.g. Friedman *et al.* 1974), based on the strong absorption theory, which provides a qualitative understanding, but it has not yet been used to analyse the experimental data and deduce nuclear penetrabilities in transfer reactions. Here is a first step in this direction.

We follow the same methods as for elastic scattering (Mohr 1979) but with a different form for the S matrix $S(l)$ in the partial wave series for the transfer amplitude $f(\theta)$. We neglect the energy change in the collision in comparison with the incident energy, as we consider transfer only to the ground state. Maximum transfer, together with rapid absorption of the incident beam, is regarded as taking place in a grazing collision at the interaction radius R for a critical angular momentum l_c and a critical scattering angle θ_c, with $\theta_c = 2\arctan(n/l_c)$. Experimentally, maximum transfer and reduction to quarter-value by absorption do not occur for quite the same value of θ_c, and in neither case is the experimental value given very well by the above relation for θ_c. We shall, however, use l_c and θ_c to denote the critical values for transfer and note that $l_c \sim kR$.

2. Form of the Angular Distributions

The transfer amplitude $f(\theta)$ is split into two additive components $f^+(\theta)$ and $f^-(\theta)$, and the value of $\sin^{\pm}\theta f^{\pm}(\theta)$ is given by the Fourier transform of $S(l)$ with respect to the variable $\lambda = l - l_c$. Friedman *et al.* (1974) take $S(l)$ to be gaussian in l and

then $\sin^{\frac{1}{2}}\theta f^{\pm}(\theta)$ is gaussian in θ. But in general the latter function is not well fitted by a gaussian except for a few degrees on either side of the peak at θ_c, whereas a good fit over the rest of the angular range is obtained with an exponential function of θ. Thus, the matrix

$$S(\lambda) = S_0 \lambda^2/(\lambda^2+\Delta^2), \tag{1}$$

with peak at $\lambda = 0$ or $l = l_c$ and half-width Δ, transforms to give

$$\sin^{\frac{1}{2}}\theta f^{\pm}(\theta) \propto \exp(-\Delta\,|\,\theta^{\pm}\,|), \tag{2}$$

where $\theta^{\pm} = \theta \pm \theta_c$. Equation (2) has a sharp peak with discontinuous slope at $\theta = \mp\theta_c$, but a sharp peak instead of a rounded peak is a price worth paying for a good fit away from the peak.

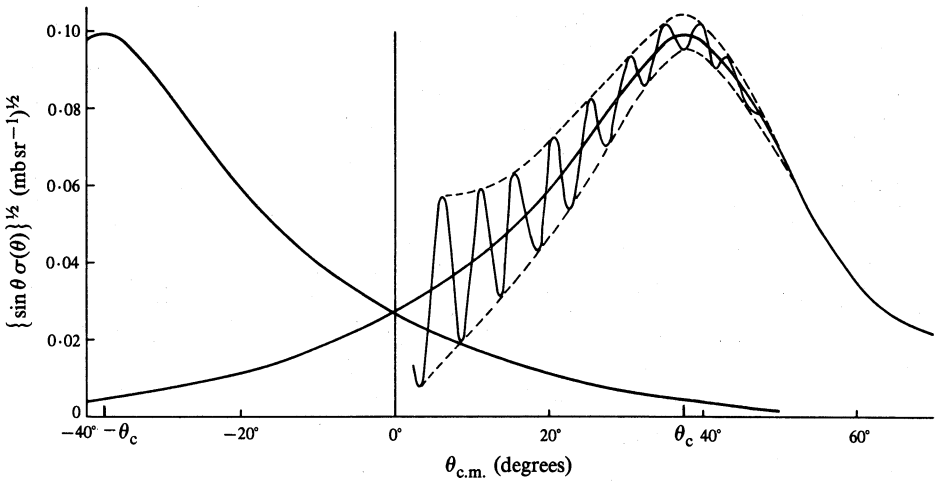

Fig. 1. Illustration of the analysis of experimental angular distributions (see Section 2).

The form (1) has the further advantage that it allows us to avoid the approximation made in the theory of replacing the summation over discrete λ by an integration over continuous λ. Thus the summation may be carried out (Gradshteyn and Ryzhik 1965, 1.445 (2)) to give

$$\sin^{\frac{1}{2}}\theta f^{\pm}(\theta) \propto \cosh\{\Delta(\pi - |\,\theta^{\pm}\,|)\}/\sinh\Delta\pi, \tag{3}$$

which differs appreciably from equation (2) only for $\Delta < 2$. If using the simple form (2) to deduce a value of Δ from an experimental angular distribution gives $\Delta < 2$, then the less simple form (3) should be used. Also the form (1) with two different values of Δ for $\lambda < 0$ and $\lambda > 0$ respectively covers the more general and realistic case of an asymmetric S (see Section 3).

Fig. 1 shows an oscillatory angular distribution for $\{\sin\theta\,\sigma(\theta)\}^{\frac{1}{2}}$ composed of two monotonic distributions (full curves) $\sin^{\frac{1}{2}}\theta f^{\pm}(\theta)$ peaked at $-\theta_c$ and θ_c respectively, with which are associated phase factors $\exp(\pm i l_c \theta)$ respectively. The $\sigma(\theta)$ distribution was calculated by Takemasa (1976) for ^{60}Ni(^{18}O,^{16}O)^{62}Ni at 65 MeV using the DWBA, and it fits fairly well the experimental curve of Baltz *et al.* (1975). The component curves are deduced by taking the sum and difference of the dashed curves drawn through the maxima and minima of the oscillatory curve. The curves have

to be terminated at a small angle, as the factor $\sin\theta$ makes them vanish at $\theta = 0$: this small limitation arises from the breakdown at small angles of the asymptotic expression used for $P_l(\cos\theta)$ in the partial wave series for $f(\theta)$.

The oscillatory form occurs only for energies well above the Coulomb barrier. For lower energies θ_c is large, the peaks in the two component distributions are further apart, and the two distributions may not overlap sufficiently at small angles to give detectable oscillations, so that one has only a bell-shaped peak.

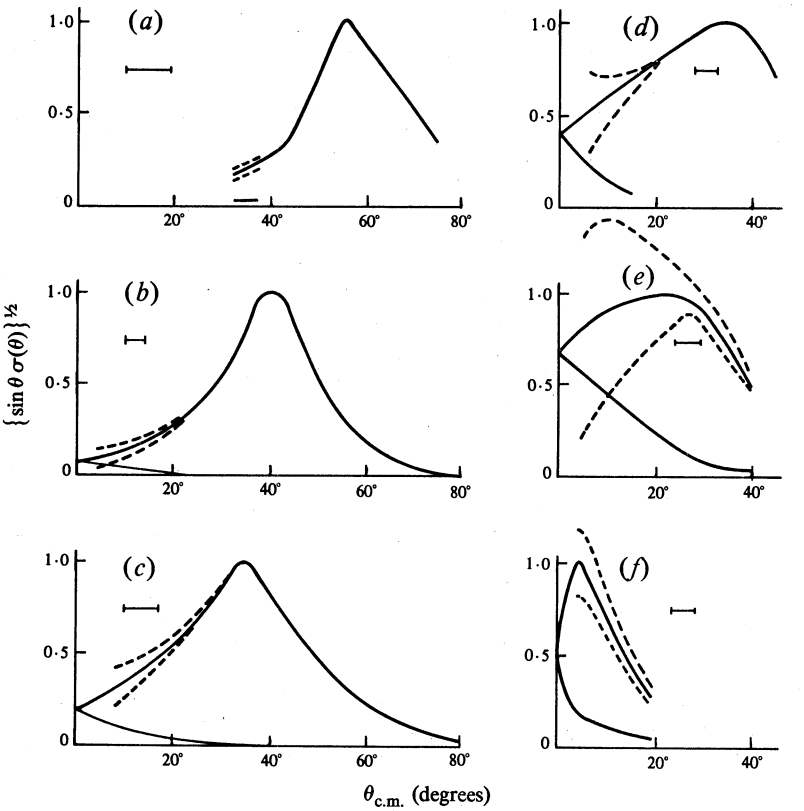

Fig. 2. Angular distributions $\{\sin\theta\,\sigma(\theta)\}^{\frac{1}{2}}$ with decreasing values of θ_c, deduced as described for Fig. 1. The oscillations contained between the dashed curves are not shown but their wavelength is indicated by the scale inserts. The full curves are normalized to a maximum value of 1. See Section 2 for references.

It is instructive to follow the changes in form as θ_c changes from large to small values, as shown in a selection of angular distributions in Fig. 2, analysed as in Fig. 1. The distributions are from experimental data in all cases except Fig. 2*b*, which is from an optical model calculation. The references are: (*a*) ^{208}Pb(^{11}B, ^{12}B)^{207}Pb at 72·2 MeV (Ford *et al.* 1974); (*b*) ^{120}Sn(^{18}O, ^{16}O)^{122}Sn at 100 MeV (Glendenning 1975, Fig. 18); (*c*) ^{48}Ca(^{16}O, ^{15}N)^{49}Sc at 56 MeV (Kovar *et al.* 1978); (*d*) ^{60}Ni(^{18}O, ^{16}O)^{62}Ni at 65 MeV (Baltz *et al.* 1975); (*e*) ^{48}Ca(^{16}O, ^{14}C)^{50}Ti at 56 MeV (Kovar *et al.* 1978); (*f*) ^{26}Mg(^{11}B, ^{12}B)^{25}Mg at 114 MeV (Paschopoulos *et al.* 1975).

Oscillations appear weakly in Fig. 2*a* at angles well below the peak, and become stronger as the peak moves to smaller angles in Figs 2*b–d*. In Figs 2*a–c* and 2*f* the

distribution is nearly exponential in form except for a few degrees on either side of the peak. In Figs 2*d* and 2*e* the distributions are more nearly gaussian and were not used in the later determination of Δ. In Fig. 2*e* the oscillations spread into the region of the peak, while in Fig. 2*f* the oscillations spread beyond the peak and are again smaller in amplitude: below 5° the precise form of the distribution cannot be determined and the form shown is partly surmise. In general, the calculated distributions are not quite symmetric about θ_c, and this may be due to the effect of refraction (see Section 4).

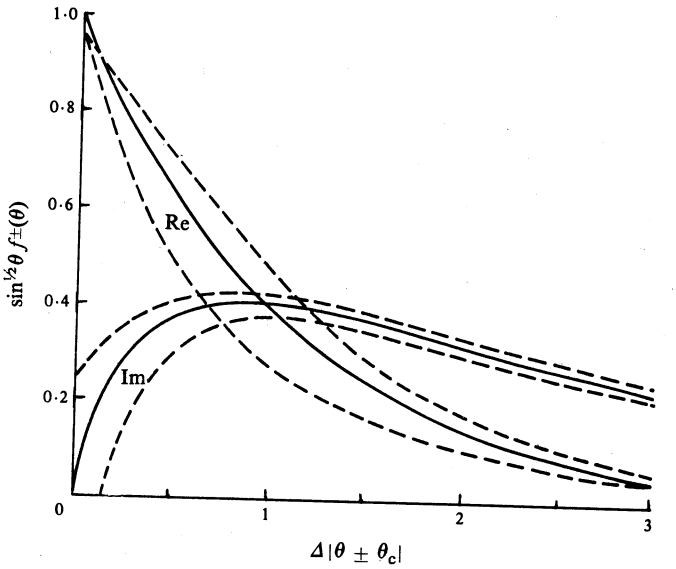

Fig. 3. Solid curves show the real and imaginary parts of $\sin^{\frac{1}{2}}\theta f^{\pm}(\theta)$ with the extreme asymmetric form (4) for $S(\lambda)$, and the nuclear phases neglected. The dashed curves show the same functions with the nuclear phases taken into account, with $\delta_0 = 1$.

3. Effect of Asymmetry of the *S* Matrix

Optical model calculations have shown that $S(\lambda)$ is not symmetric about the value $\lambda = 0$ (Glendenning 1975). An asymmetric $S(\lambda)$ may be constructed from two half-peaks with the same height but different half-widths. Thus, the form

$$S(\lambda) = 0, \qquad \lambda < 0, \tag{4a}$$

$$= \tfrac{1}{2}S_0 \Delta^2/(\lambda^2+\Delta^2), \qquad \lambda > 0, \tag{4b}$$

gives (Gradshteyn and Ryzhik 1965, 3.723 (1) and (2))

$$\sin^{\frac{1}{2}}\theta f^{\pm}(\theta) \propto \exp(-\Delta|\theta^{\pm}|) + i\pi^{-1}\{\exp(-\Delta|\theta^{\pm}|)\,\overline{\mathrm{Ei}}(\Delta|\theta^{\pm}|) - \exp(\Delta|\theta^{\pm}|)\,\mathrm{Ei}(-\Delta|\theta^{\pm}|)\}. \tag{5}$$

The values of the real and imaginary parts of this expression are shown by the full curves in Fig. 3. Then the value of $\sin^{\frac{1}{2}}\theta f^{\pm}(\theta)$ for an S of the form (1) with $\Delta = \Delta_1$ on one side of the peak and $\Delta = \Delta_2$ on the other side is obtained by taking the sum of the real parts and the difference of the imaginary parts for $\Delta_1|\theta^{\pm}|$ and

$\Delta_2|\theta^{\pm}|$. The total real part is approximately equal to the real part for symmetric S with $\Delta = \frac{1}{2}(\Delta_1+\Delta_2)$. The total imaginary part becomes appreciable only at angles θ well away from the peak at θ_c and so has the effect of slightly flattening out the angular distribution there.

One of the approximations in the theory is to take the term $(2l+1)^{\frac{1}{2}}$ in the partial wave series to have the constant value $(2l_c+1)^{\frac{1}{2}}$. The effect of allowing for the variation of this term can be imitated by increasing the asymmetry of S. Another of the approximations is to take the difference between successive Coulomb phases to be $\arctan(n/l_c)$ instead of the exact value $\arctan(n/l)$, and this was found to involve errors of about 20% in the value of Δ. This is unfortunate but the approximation has long been used and cannot be avoided.

4. Effect of Refraction

We now take account of refraction, which we found to be of fundamental importance for a satisfactory account of elastic collisions. As before we introduce the nuclear phases δ_l with the parametrization $\delta_l = \delta_0\{1-S_{WS}(l)\}$, where $S_{WS}(l)$ is of Woods–Saxon form with width parameter Δ, and calculate numerically the change this produces.

The change is found to depend only on the product $\Delta\theta^{\pm}$ when $\Delta > 2$, and it is approximately proportional to δ_0 for $\delta_0 < 1$, increasing less and less rapidly as δ_0 increases beyond 1. The sign of the change depends on the signs of $\theta^{\pm}$ and δ_l, as seen by considering the spiral formed by the amplitude–phase diagram for the partial wave series, as explained for elastic scattering (Mohr 1979): the effect of the δ_l is either to increase or decrease the distance between the ends of the section of spiral. The values of the real and imaginary parts of $f^-(\theta)$ are decreased for $\theta > \theta_c$ and increased for $\theta < \theta_c$, those for $f^+(\theta)$ are increased for $\theta > -\theta_c$ and decreased for $\theta < -\theta_c$: the changes are thus symmetric about $\theta = 0$. The changed values are shown by the dashed lines in Fig. 3 for $\Delta > 2$.

The result is to increase the slope of the $\log|f(\theta)|$ versus θ curve from Δ to Δ^- (say) on the large-angle side of the peak at θ_c and decrease it from Δ to Δ^+ on the small-angle side. Also, Δ is nearer to the geometric mean of Δ^+ and Δ^- than to the arithmetic mean. The change in Δ due to refraction is much smaller for transfer reactions than for elastic scattering. Thus for $\delta_0 = 1$, $\Delta^-/\Delta^+ \sim 1{\cdot}3$ for transfer, whereas it may be as large as 3 for elastic scattering.

5. Analysis of Angular Distributions

Values of Δ obtained from analysis of angular distributions are shown in Fig. 4. They are plotted as a function of $k-k_B$ where k_B is the value of Δ for the top of the Coulomb barrier, and indeed the values of Δ do drop near $k-k_B = 0$. The dashed curves link points for a reaction which has been studied for more than one energy. The letters against the experimental points refer to the references given below [in square brackets].

Most of the data are for the nuclei O, N and C incident on heavier target nuclei, and we consider first the heaviest target nuclei, then the less heavy ones, and so on. Olmer *et al.* (1978) [O] have studied the reaction $^{208}Pb(^{16}O,^{15}N)^{209}Bi$ at 313, 217, 139 and 104 MeV, while Dar (1965)[Da] has studied the reaction $^{197}Au(^{14}N,^{13}N)^{198}Au$ at 133, 126, 120, 110, 102 and 90 MeV. In both experiments the progression of theoretical curves of best fit to the experimental points was used to help overcome the

difficulty of an insufficiency of such points for a satisfactory determination of Δ. These curves show only the bell-shaped peak.

Ford *et al.* (1974) [Fo] have studied the four reactions occurring with ^{11}B on ^{208}Pb at 72 MeV and involving either neutron or proton transfer, obtaining curves in which a couple of small-angle oscillations begin to appear. The values obtained for Δ were nearly the same in the four reactions and the mean is used in Fig. 4. Curves of similar form at slightly smaller angles have been obtained for somewhat lighter target nuclei by Sherwood *et al.* (1978) [S] for ^{48}Ti(^{16}O, ^{15}N)^{49}V at 50 MeV, and by Essel *et al.* (1979) [E] for ^{54}Fe(^{18}O, ^{17}O)^{55}Fe at 56 MeV and ^{54}Fe(^{17}O, ^{16}O)^{55}Fe at 59 MeV, and the mean Δ for each study is used in Fig. 4.

Curves for slightly less heavy target nuclei have been obtained from optical model calculations, and these have the advantage of showing the main peak together with oscillations extending to zero scattering angle: Glendenning (1975) [Gl] has considered ^{120}Sn(^{18}O, ^{16}O)^{122}Sn at 160 and 100 MeV, Takemasa (1976) [T] ^{60}Ni(^{18}O, ^{16}O)^{62}Ni at 65 MeV, and Garrett *et al.* (1975) [Ga] ^{27}Al(^{32}S, ^{31}P)^{28}Si at 100 MeV. The curves of Glendenning and of Garrett *et al.* use optical model parameters which have no experimental basis, and they show considerable variation with potential well depth (we used Figs 24 and 18 of Glendenning), while the curve of Takemasa is a fairly good fit to the experimental points of Baltz *et al.* (1975).

We come now to still lighter target nuclei. Kovar *et al.* (1978) [K] have investigated the four reactions resulting from ^{16}O on ^{48}Ca at 56 MeV. For the (^{16}O, ^{17}O) reaction they obtained the bell-shaped peak and strong oscillations at smaller angles, while for the (^{16}O, ^{15}N) reaction oscillations are hardly visible, and they attributed this behaviour to greater kinetic mismatch in this reaction: the two reactions give nearly the same value of Δ and we have taken the mean in Fig. 4. For the (^{16}O, ^{14}C) reaction, there are marked oscillations even beyond the bell-shaped peak, but the curve obtained for $\sin^{\frac{1}{2}}\theta f^-$ has a maximum too broad to be fitted with an exponential form, as already mentioned in Section 4. For (^{16}O, ^{14}N) the error bars are too large to show definite maxima and minima and so allow a separation of f^+ and f^-. The angular distribution for (^{16}O, ^{14}C) has approximately the form of the square of a Bessel function of argument $(l+\frac{1}{2})\theta$ (Henning *et al.* 1974), and represents the case where the bell-shaped peak and the forward oscillations overlap; it is a form which occurs in all cases when θ_c is small, as for pairs of light nuclei at not too low energies. The transition from bell-shaped peak to oscillations at smaller angles is shown by Bond *et al.* (1973) [Bo] for ^{40}Ca(^{13}C, ^{12}C)^{41}Ca at 40, 48, 60 and 68 MeV, and the change in Δ is indicated in Fig. 4 by the dashed curve through the middle of the group of four points labelled Bo.

In the rest of the cases now to be discussed, the value of θ_c is small, so the bell-shaped peak has disappeared, and the forward maxima and minima are as indicated in Fig. 2*f*, gradually diminishing in amplitude with increasing angle. It may be impossible to determine $\sin^{\frac{1}{2}}\theta f^+(\theta)$, and hence Δ^+ with any accuracy, but usually we have $\Delta^+ \simeq \Delta^-$ in this region. Dehnhard *et al.* (1979) [De] have studied ^{48}Ca(^{18}O, ^{16}C)^{50}Ti at 102 MeV. Paschopoulos *et al.* (1975) [P] have studied the four possible cases of single nucleon transfer for 114 MeV ^{11}B on ^{26}Mg, and the mean of four similar values of Δ is plotted in Fig. 4. Clark *et al.* (1979) [C] have studied ^{24}Mg(^{16}O, ^{12}C)^{28}Si at 72·5, 67·0, 65·0 and 62·5 MeV: these curves are all similar, but the value of Δ was taken from the 67·0 MeV curve, as this covers the widest angular range. DeVries (1973) [DV] has studied ^{14}N on ^{11}B with proton pickup and

with proton stripping at 41, 77 and 113 MeV; the pair of values of Δ so obtained at each energy have been averaged for Fig. 4 and the three points linked by a dashed curve. Nair *et al.* (1975) [N] have studied 100 MeV ^{10}B on ^{12}C, ^{14}N and ^{16}N, and also 155 MeV ^{14}N on ^{12}C and ^{16}O, with single nucleon transfer in each case; the averaged values of Δ at each of the two energies have been plotted and linked by a dashed curve. Fulmer *et al.* (1979) [Fu] have studied 93·8 MeV ^{12}C on ^{12}C with neutron and with proton transfer, from which the mean Δ has been taken.

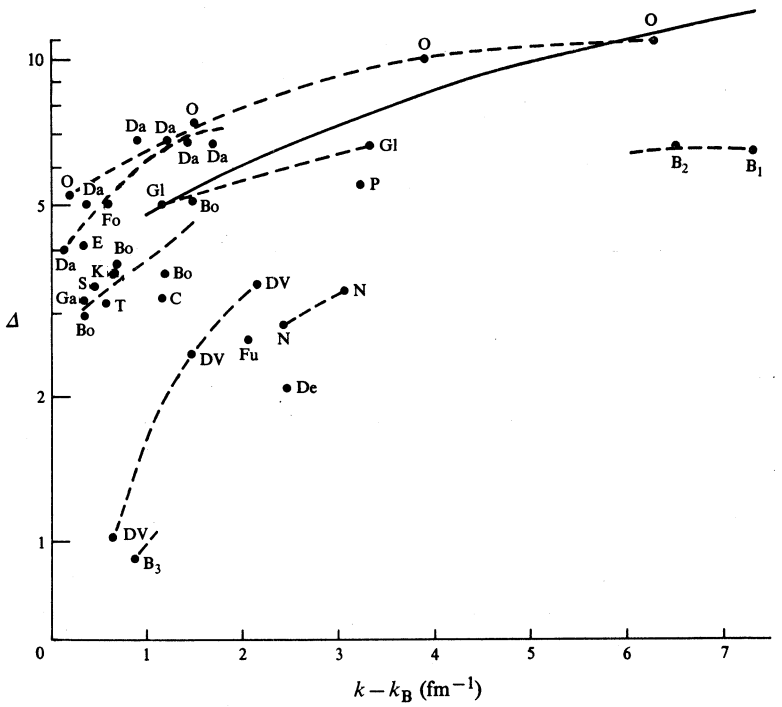

Fig. 4. Values for the width parameter Δ of the S matrix (1) for different values of $k-k_B$. The dashed curves link values for the same reaction at different energies. The solid curve is for $\pi\Delta_{WS}$ (see Section 7). Details of all the data plotted, with references, are given in Section 5.

Finally we discuss three recent experiments on the (p, d) reaction, the first two with isotopic target nuclei. Bauer *et al.* (1980) [B_1] have studied 800 MeV protons on ^{13}C, and Baker *et al.* (1974) [B_2] 700 MeV protons on ^{12}C; the two corresponding values of Δ are linked by a dashed curve. Barbopoulos *et al.* (1979) [B_3] have studied 33 MeV protons on ^{76}Se. The points B_1, B_2 and B_3 mark out a curve which is steeper than the other dashed curves, but its path is uncertain. For the above light nuclei at low energies Δ is small, so only a small number of values of l contribute to the reaction: in an extreme case the angular distribution may be dominated by a single value of l (Paul *et al.* 1978).

6. Results of the Analysis

All the results of the analysis are presented in Fig. 4. The values of Δ are seen to increase with $k-k_B$ and with the size of the nuclei. The latter dependence differs from that for elastic collisions where there is little variation in Δ_{WS} with nuclear size.

The biggest variation in Δ with nuclear size occurs for small $k-k_B$, but here the values of k_B, and hence $k-k_B$, are unreliable because the barrier height was calculated from the crude formula $Z_1 Z_2 e^2/(R_1+R_2)$ with $R_{1,2} = r_0 A_{1,2}^{\frac{1}{3}}$ for simplicity, taking $r_0 = 1{\cdot}2$ fm in all cases. One should calculate the barrier penetrability for energies near the top of the barrier, and establish a better basis of comparison of Δ values at the lower energies.

At the higher energies we have a more meaningful basis of comparison. The colliding nuclei behave more like particles, and their angular momentum l is proportional to their separation r (in particular $l_c = kR$), so the S matrix which gives the distribution of l values also gives approximately the distribution of r values. Hence the width Δ of the l distribution is approximately k times a, the width of the r distribution for nuclei involved in transfer; so $a \simeq k^{-1}$ (the slope of the Δ versus $k-k_B$ curve), with Δ plotted on a linear scale, and not a log scale as used in Fig. 4. Here the quantity a refers to the surface diffuseness of the transition density, which is not the same as the mass density.

The present data are too fragmentary for drawing any firm conclusions about the slope of the Δ versus $k-k_B$ curves at larger k; in fact the slopes, and therefore a, may not be independent of energy. It seems however that the slopes, and hence a, increase with decreasing size of the nuclei: this is particularly evident for the curve $B_1 B_2 B_3$ for (p, d) reactions in Fig. 4. In fact Glendenning (1975) has already concluded that deep penetration is preferred in transfer reactions, and has discussed this in terms of the 'pocket' in the effective nuclear potential which occurs only if $Z_1 Z_2$ is small enough. The increase in penetration does not, however, appear to be large, and by no more than a factor of about 2 over the whole range of nuclei. The range of values of a obtained from DWBA fits to transfer angular distributions is about the same, but does not show any systematic difference between large and small nuclei.

More definite conclusions cannot be obtained from the present inadequate experimental data: the points on the curves are sometimes too widely spaced and too few in number, and the observations usually taken at too low energies.

The optical model, with its arbitrary parameters determined only by best fit with experiment at a single energy, is no longer providing fresh information and understanding. The S-matrix approach, based on the philosophy of working from the outside of the nucleus inwards instead of vice versa, should do better, as soon as experiments are performed systematically for each pair of nuclei over a range of energies.

7. Circumstances for Strong Coupling between Elastic Scattering and Transfer

For a close similarity between the angular distributions for elastic scattering and transfer, the latter should be large at small angles so that coupling to the elastic scattering in a two-stage process will cause it to follow the elastic scattering over the angular range. There is no similarity when θ_c is large, at the energies used so far, for then the transfer distribution has a broad peak at largish angles and a low intensity at small angles, features not seen in the elastic scattering. There is the possibility of a similarity when θ_c is quite small, for then the two distributions are largest at small angles and fall off with increasing angle. There are only weak oscillations, and $\Delta^- \simeq \Delta^+ \simeq \Delta$ for both distributions, which are of the form $\exp(-\pi\Delta_{WS}\theta^-)$ and $\exp(-\Delta\theta^-)$ respectively. These two quantities will be the same when $\pi\Delta_{WS} = \Delta$. A plot of Δ_{WS} is shown in Fig. 4 by the full curve, and this curve is close to values of Δ

for large nuclei only. But for large nuclei, transfer will be small at small angles except at much higher energies than in the present experiments. To show the existence of strong coupling requires experiments to be extended to smaller angles and higher energies.

Now there is another circumstance in which the two distributions may have a similar form, namely when $\pi\Delta_{WS} \simeq \Delta$ and both are particularly small—a situation called a small l window by Rowley (1980)—so that the two distributions are dominated by the same small group of $P_l(\cos\theta)$. This has been seen to occur only for a few light nuclei. Rowley refers specifically to ^{16}O on ^{16}O. Fig. 4 shows a particularly small Δ for ^{14}N on ^{11}B at the lowest energy 41 MeV (DeVries 1973), while Fig. 4 of our previous paper (Mohr 1979) shows a particularly small $\pi\Delta_{WS}$ of similar magnitude for 15 MeV ^{12}C on ^{14}C (Delic 1975) and 52 MeV ^{18}O on ^{16}O (Reisdorf *et al.* 1975). In the case of ^{14}N on ^{11}B with transfer we have the largest slope of the Δ versus $k-k_B$ curve, and so the deepest penetration into the nuclear field, which therefore tends to dominate all the channels and couple them.

References

Baker, S. D., *et al.* (1974). *Phys. Lett.* B **52**, 57.
Baltz, A. J., Bond, P. D., Garrett, J. D., and Kahana, S. (1975). *Phys. Rev.* C **12**, 136.
Barbopoulos, L. O., Gebbie, D. W., Nurzynski, J., Boraru, M., and Hollas, C. L. (1979). *Nucl. Phys.* A **331**, 502.
Bauer, T. S., *et al.* (1980). *Phys. Rev.* C **21**, 757.
Bond, P. D., *et al.* (1973). *Phys. Lett.* B **47**, 231.
Clark, P., *et al.* (1979). ANU Research School of Physical Sciences, Ann. Rep., p. G43.
Dar, A. (1965). *Phys. Rev.* B **139**, 1193.
Dehnhard, D., Saathoff, W., Bhatia, T. S., Wannebo, K., and Wiedner, C.-A. (1979). *Z. Phys.* A **291**, 71.
Delic, G. (1975). *Phys. Rev. Lett.* **34**, 1468.
DeVries, R. M. (1973). *Phys. Rev.* C **8**, 951.
Essel, H., Rehm, K. E., Bohn, H., Körner, H. J., and Spieler, H. (1979). *Phys. Rev.* C **19**, 2224.
Ford, J. L. C., *et al.* (1974). *Phys. Rev.* C **10**, 1429.
Friedman, W. A., McVoy, K. W., and Shuy, G. W. T. (1974). *Phys. Rev. Lett.* **33**, 308.
Fulmer, C. B., *et al.* (1979). *Phys. Rev.* C **20**, 670.
Garrett, J. D., *et al.* (1975). *Phys. Rev.* C **12**, 489.
Glendenning, N. K. (1975). *Rev. Mod. Phys.* **47**, 659.
Gradshteyn, I. S., and Ryzhik, I. M. (1965). 'Tables of Integrals, Series and Products' (Academic: New York and London).
Henning, W., Kovar, D. G., Zeidman, B., and Erskine, J. R. (1974). *Phys. Rev. Lett.* **32**, 1015.
Kovar, D. G., *et al.* (1978). *Phys. Rev.* C **17**, 83.
Mohr, C. B. O. (1979). *Aust. J. Phys.* **32**, 541.
Nair, K. G., *et al.* (1975). *Phys. Rev.* C **12**, 1575.
Olmer, C., *et al.* (1978). *Phys. Rev.* C **18**, 205.
Paschopoulos, I., *et al.* (1975). *Nucl. Phys.* A **252**, 173.
Paul, M., *et al.* (1978). *Phys. Rev. Lett.* **40**, 1310.
Reisdorf, W. N., Lau, P. H., and Vandenbosch, R. (1975). *Nucl. Phys.* A **253**, 490.
Rowley, N. (1980). *J. Phys.* G **6**, 697.
Sherwood, G. B., Erb, K. A., Hanson, D. L., Ascuitto, R. J., and Bromley, D. A. (1978). *Phys. Rev.* C **18**, 2574.
Takemasa, T. (1976). *Phys. Rev.* C **13**, 2343.

Manuscript received 30 July 1980, accepted 29 October 1980